

**Stem Cell Reports, Volume 5**

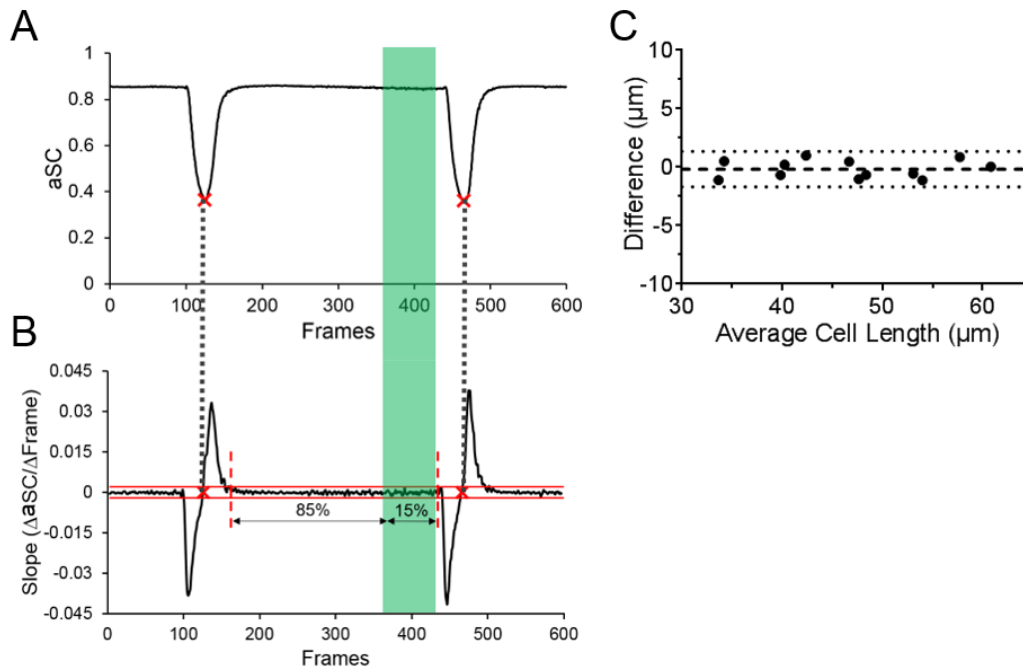
**Supplemental Information**

**Integrated Analysis of Contractile Kinetics, Force  
Generation, and Electrical Activity in Single Human Stem  
Cell-Derived Cardiomyocytes**

**Jan David Kijlstra, Dongjian Hu, Nikhil Mittal, Eduardo Kausel, Peter van der Meer,  
Arman Garakani, and Ibrahim J. Domian**

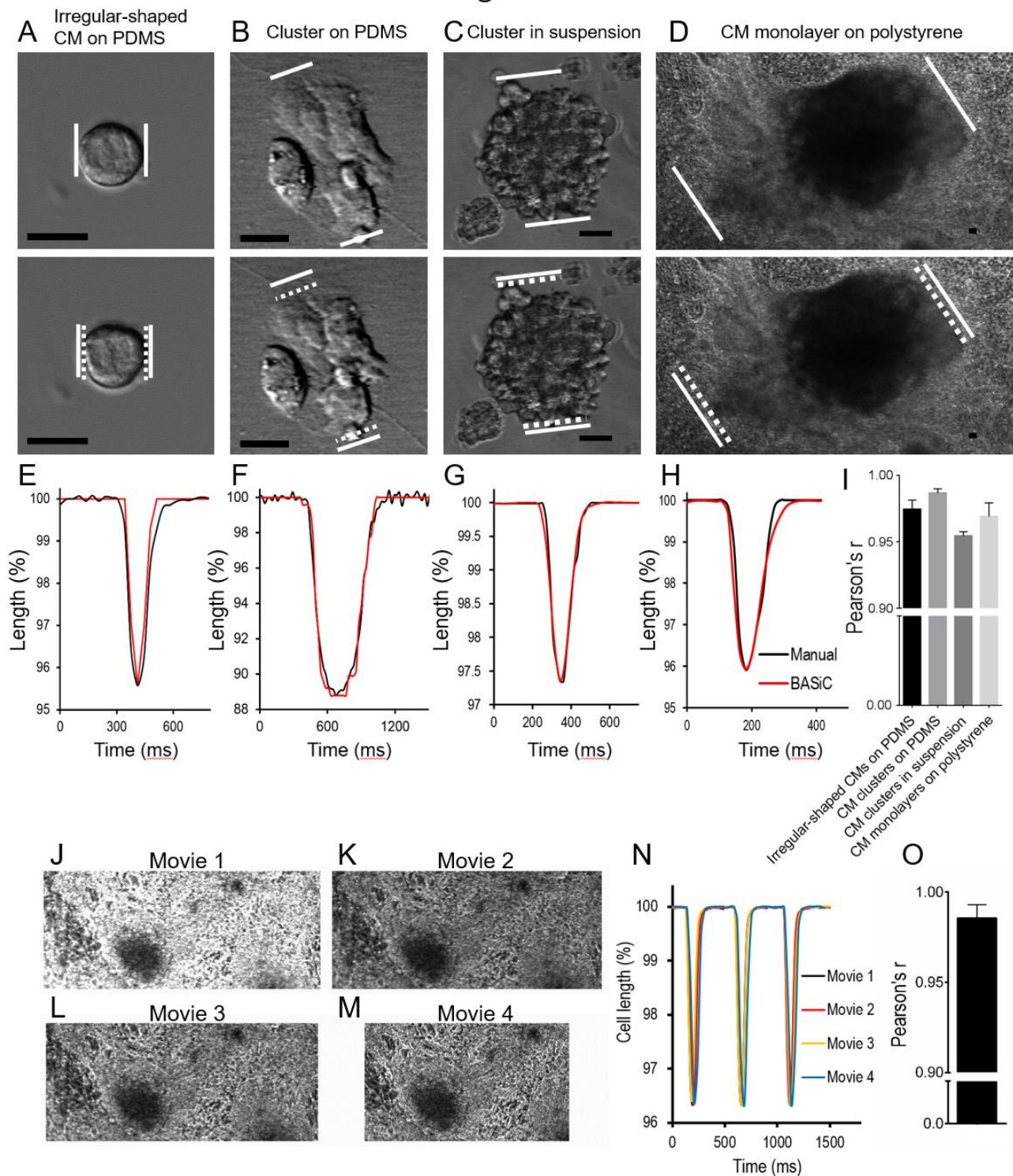
## Supplemental Figures

### Figure S1



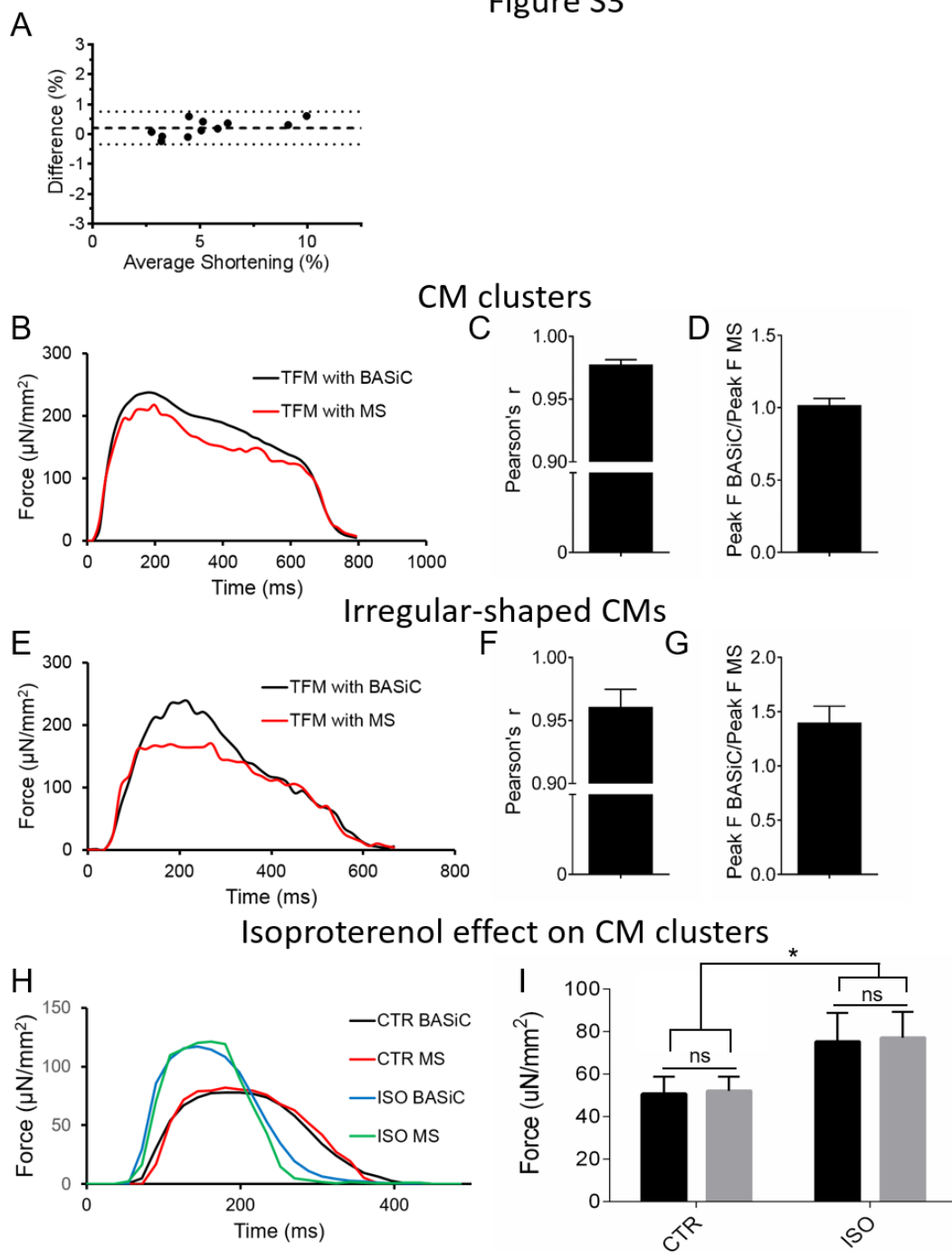
**Figure S1. Selection of Pre-contractile Frames and Reliability of Cell Length Measurements, Related to Figure 2.** (A) Graph of averaged SC (aSC) of all frames over frame number for Movie S1. Red crosses mark the points of maximum contraction (local minimum). (B) Slope ( $\Delta aSC/\Delta Frame$ ) of the rolling five-point linear fit line. The inter-contractile interval is marked by dashed red lines and defined as frames with a deviation of slope from 0 of less than 5% of the minimum slope as indicated by red lines. Frames in the terminal 15% of the inter-contractile interval are defined as pre-contractile marked by the green shaded area. The dotted black lines show the correlation between maximum contraction points in aSC and slope. (C) Bland-Altman graph of average cell length measurement of two observers plotted against the difference between measurements. Cell length measurements between observers were highly similar with a mean difference (dashed line) of  $0.17\mu m$  (not significantly different from 0;  $P = 0.45$ ) and 95% limits of agreement (dotted lines) of  $-1.69\mu m$  to  $1.35\mu m$ .  $n = 12$  cells from 3 independent experiments.

Figure S2



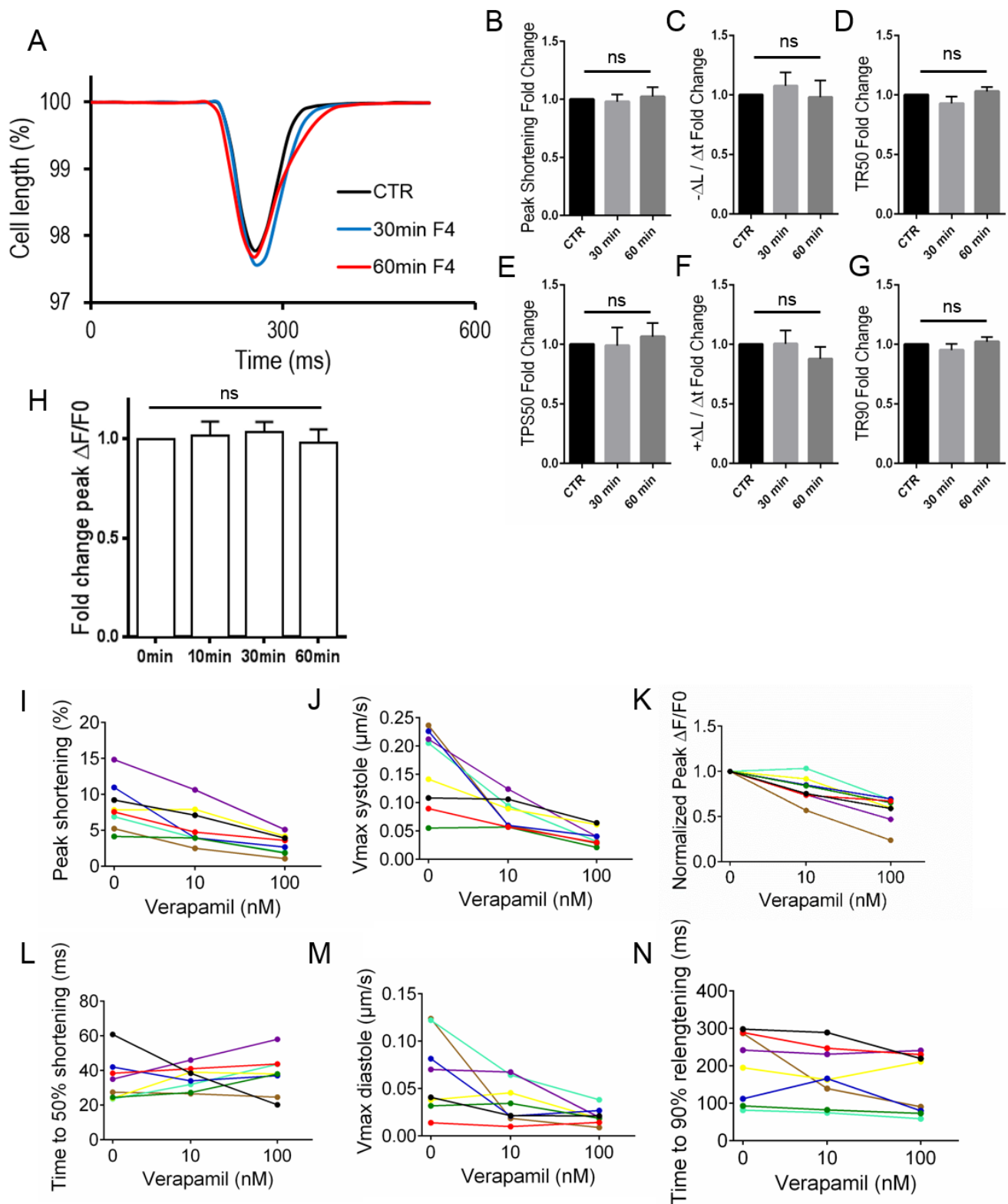
**Figure S2. Validation of BASiC for Irregular-shaped CMs, CM Clusters, and Monolayers and Different Movie Acquisition Settings, Related to Figure 3.** (A-D) Comparison of a representative irregular shaped hESC-CM on PDMS, hESC-CM cluster on PDMS, hESC-CM cluster in suspension and hESC-CM monolayer on polystyrene in a relaxed (top panel) vs. a contracted (bottom panel) state. Solid white lines represent position of cell structure edges in relaxed state. Dotted white lines represent position of cell structure edges in contracted state. Scale bars, 20  $\mu\text{m}$ . (E-H) Contraction curves generated by manual measurement (black line), and BASiC (red line) of the representative cell/cluster/monolayer. (I) Pearson's correlation coefficient (Pearson's  $r$ ) between contraction curves generated by manual measurement and BASiC of cells/clusters/monolayers.  $n =$  at least 6 from 3 independent experiments for all groups. Data are represented as mean  $\pm$  SE. (J-M) Four movies of the same hESC-CM monolayer on polystyrene acquired with a variety of settings for frame rate, resolution and pixel saturation. Movie 1: 100 fps, resolution 2.52  $\mu\text{m}/\text{px}$ , oversaturated lighting. Movie 2: 100 fps, resolution 2.52  $\mu\text{m}/\text{px}$ , normal lighting. Movie 3: 55 fps, resolution 2.52  $\mu\text{m}/\text{px}$ , normal lighting. Movie 4: 30 fps, resolution 1.26  $\mu\text{m}/\text{px}$  and normal lighting. (N) Contraction curves generated by BASiC of Movies 1-4 acquired under different settings show a high degree of similarity. (O) Pearson's  $r$  between contraction curves of movies of hESC-CM monolayers acquired with a variety of settings as described above.  $n = 5$  from 3 independent experiments. Data is represented as mean  $\pm$  SE. See also Movies S6, S7 and S8.

Figure S3



**Figure S3. Correlation of Bead Movement and Cell Movement, Force Calculations for CM Clusters and Irregular-shaped CMs, and Isoproterenol Effect on CM Clusters, Related to Figure 4.** (A) Fluorescent microsphere movement accurately translates into CM shortening. Bland-Altman graph of average of microsphere movement measurement and CM shortening measurement. Microsphere movement and CM shortening correlate closely with a mean difference (dashed line) of 0.16% (not significantly different from 0;  $P = 0.08$ ) and 95% limits of agreement (dotted lines) of -0.35% to 0.68%.  $n = 11$  cells from 3 independent experiments. (B) Plot of contractile force of a hESC-CM cluster calculated by Traction Force Microscopy (TFM) using BASiC overlaid with force calculated by TFM using fluorescent microspheres (MS). (C) Pearson's  $r$  between contraction curves generated by the two methods.  $n = 11$  CM clusters from 3 independent experiments. (D) Ratio of peak force calculated by TFM with BASiC over peak force calculated by TFM with MS. (E) Plot of contractile force of a hESC-CM cluster calculated by TFM using BASiC overlaid with force calculated by TFM using MS. (F) Pearson's  $r$  between contraction curves generated by the two methods.  $n = 6$  cells from 3 independent experiments. (G) Ratio of peak force calculated by TFM with BASiC over peak force calculated by TFM with MS. (H) Plot of contractile force of a hESC-CM cluster calculated by TFM using BASiC overlaid with force calculated by TFM using fluorescent microspheres (MS) before (CTR) and after (ISO) application of 100nM isoproterenol. (I) Average force as calculated by TFM with BASiC and MS before and after application of ISO shows no significant differences between the two methods before and after pharmacological intervention.  $n = 7$  CM clusters from 3 independent experiments. \* $P < 0.05$ . Data are represented as mean  $\pm$  SE.

Figure S4



**Figure S4. Fluoro-4AM Effect and Signal Consistency, and Intercell Variability in Response to Verapamil, Related to Figure 5.** (A) Representative contraction curves of a single hESC-CM before treatment and 30 min and 60 min after treatment with 0.5  $\mu\text{M}$  Fluoro-4AM (F4) calcium transient indicator. (B-G) Fold change in peak shortening, time to 50% peak shortening (TPS50), maximum shortening velocity ( $-\Delta L/\Delta t$ ), maximum relengthening velocity ( $+\Delta L/\Delta t$ ), time to 50% relengthening (TR50) and time to 90% relengthening (TR90) of cells 30 min and 60 min after treatment with 0.5  $\mu\text{M}$  Fluoro-4AM compared to baseline.  $n = 6$  cells from 3 independent experiments. (H) Fold change in peak intracellular fluorescence signal of hESC-CMs loaded with 0.5  $\mu\text{M}$  Fluoro-4AM. Measurements were taken at 0, 10, 30 and 60 minutes.  $n = 10$  cells from 3 independent experiments. Data are represented as mean  $\pm$  SE. (I-N) Intercellular variability in contractile characteristics of hESC-CMs at baseline and in response to treatment with 10nM and 100nM verapamil. Each colored line represents one cell.



Figure S5

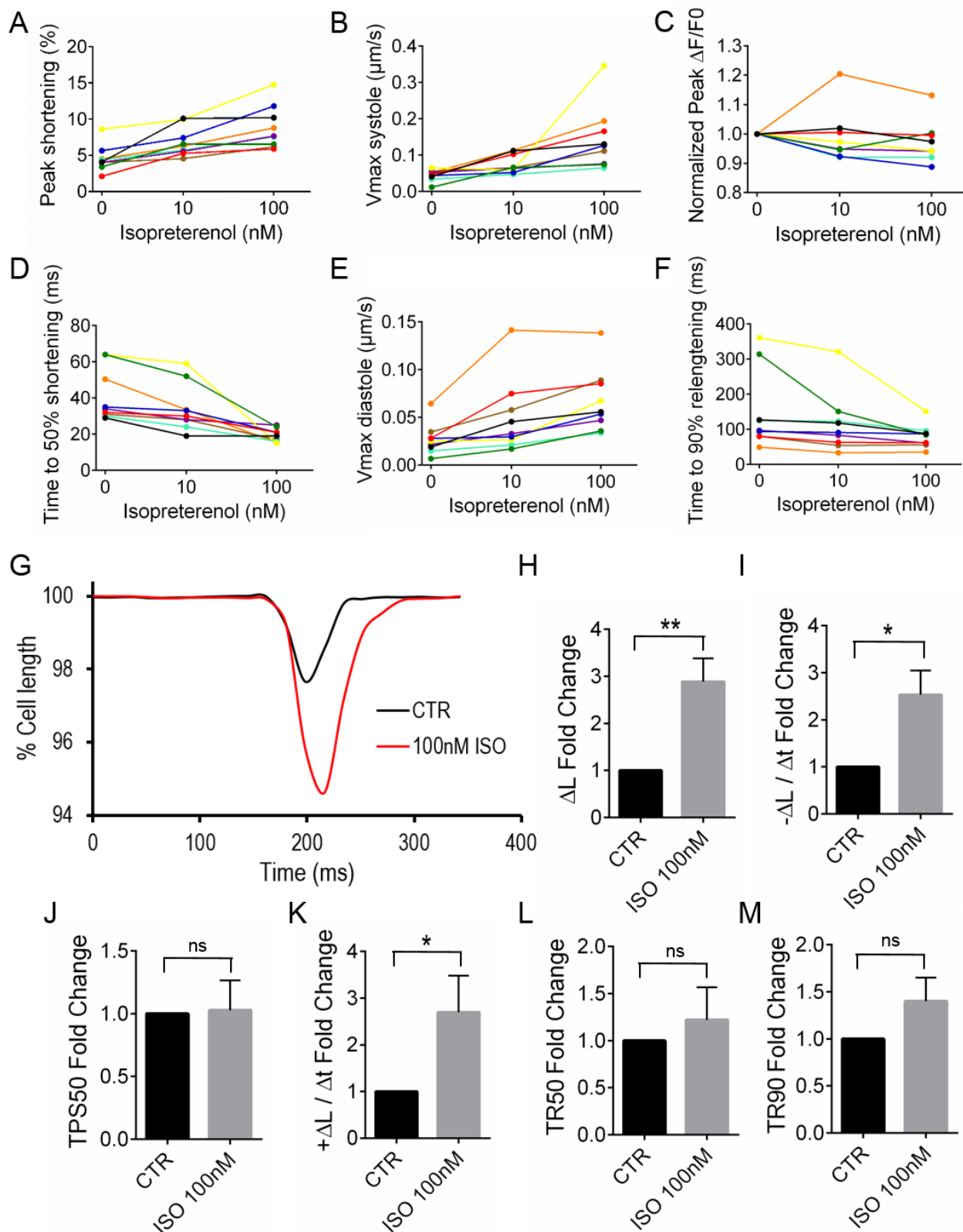


**Figure S5. Intercell Variability of hESC-CMs in Response to Isoproterenol and Effect of Isoproterenol on Adult CMs, Related to Figure 6.** (A-F) Intercellular variability in contractile characteristics of hESC-CMs at baseline and in response to treatment with 10nM and 100nM isoproterenol. Each colored line represents one cell. (G) Representative contraction curves of a single isolated field-stimulated adult CM before and after treatment with 100nM isoproterenol. (H-M) Fold change in peak shortening ( $\Delta L$ ), maximum shortening velocity ( $-\Delta L/\Delta t$ ), time to 50% peak shortening (TPS50), maximum relengthening velocity ( $+\Delta L/\Delta t$ ), time to 50% relengthening (TR50) and time to 90% relengthening (TR90) of adult CMs after treatment with 100nM isoproterenol compared to baseline.  $n = 7$  cells from 3 independent experiments. Data are represented as mean  $\pm$  SE. \* $P < 0.05$ ; \*\* $P < 0.01$ .

## Supplemental Experimental Procedures

### Normalization of Contraction Curve

The baseline adjusted similarity comparison (BASiC) index and frame numbers of the BASiC contraction curve were normalized to respectively percentage of maximum cell length and time. For this purpose, manual cell length measurements were performed in Fiji (Schindelin et al., 2012) over the longitudinal axis of the cell at the last frame prior to contraction ( $length_{max}$ ) and the peak shortening frame ( $length_{min}$ ). These manual measurements were used in the following equation to normalize BASiC to cell length:

$$Length = length_{max} \left(1 - \frac{1 - SC/SC_{max}}{NR}\right)$$

The  $SC_{max}$  was defined as the average SC of the previously selected pre-contraction frames.  $SC_{min}$  is the SC value at the peak shortening frame. The Normalization Ratio (NR) is a measure of the relative change in SC compared to the relative change in length during a contraction and is defined as:

$$NR = \frac{1 - SC_{min}/SC_{max}}{1 - length_{min}/length_{max}}$$

### Traction Force Microscopy without Fluorescent Microspheres

To calculate contractile force generated by cardiomyocytes on flexible substrates with a static mechanical model we make the following assumptions: 1.) The cell is rectangular, and contracts along one of its directions, without any lateral impediment. 2.) The stiffness of the cell is negligible compared to the stiffness of the gel to which the cell is attached. 3.) The shearing forces are symmetric with respect to the center, that is, they point in opposite directions and cancel in the aggregate. 4.) The shearing traction distribution is assumed to be governed by Boussinesq's law  $\sim 1/\sqrt{1 - (\frac{x}{a})^2}$ , where  $a$  is the half-length of the cell.

For the 5kPa PDMS used in these experiments the Poisson's ratio ( $\nu$ ) was set to 0.5, the mass density of the gel ( $\rho$ ) was set to 1.08 g/cm<sup>3</sup>, and the shear wave velocity ( $C_s$ ) was set to 200.8 cm/s. The shear modulus ( $G$ ) was then calculated as:

$$G = \rho C_s^2$$

We sub-divide the rectangular cell of dimensions  $2a \times 2b$  into narrow rectangles of width  $\Delta x$ . Consider a rectangular load of dimension  $\Delta x \times 2b$  and magnitude  $q_x$  applied at the free surface of the half-space, with its sides oriented parallel to the  $x, y$  axes. It can be shown that the horizontal displacement at the center of the load is given by

$$u_{ox} = \frac{2q_x}{\pi G} \left\{ I_1\left(\frac{1}{2}\Delta x, b\right) + \nu \left[ I_2\left(\frac{1}{2}\Delta x, b\right) - I_1\left(\frac{1}{2}\Delta x, b\right) \right] \right\},$$

Where

$$I_1(a,b) = \frac{1}{2} \int_0^{2b} \int_0^{2a} \frac{dx dy}{(x^2 + y^2)^{1/2}} = a \sinh^{-1} \frac{b}{a} + b \sinh^{-1} \frac{a}{b}$$

$$I_2(a,b) = \frac{1}{2} \int_0^{2b} \int_0^{2a} \frac{x^2 dx dy}{(x^2 + y^2)^{3/2}} = b \sinh^{-1} \frac{a}{b},$$

We consider next the case of contact stresses underneath the cardiomyocyte that follow the Boussinesq law:

$$q_x = \frac{2bq_0}{\sqrt{1 - \left(\frac{x}{a}\right)^2}}$$

The displacement elicited by each narrow slit at any location is then evaluated via equation (1), scaling the intensity  $q_0$  of the load so that the total elongation of the cell equals the cell's length (i.e. unit strain). Finally, the force needed to accomplish that strain is computed as

$$P_x = q_0 2b \int_0^a \frac{1}{\sqrt{1 - \left(\frac{x}{a}\right)^2}} dx = \pi q_0 ab .$$

### Isolation of Adult Mouse Cardiomyocytes

Mouse hearts from adult C57BL/6 mice were perfused with a Langendorff apparatus as previously reported (Graham et al., 2013). Briefly, a 12-gauge mouse feeding needle was inserted into the aorta and the heart was subsequently perfused for 18 min at a rate of 1 ml min<sup>-1</sup> with Tyrode Buffer supplemented with 5.5 mM D-(+)-Glucose (Sigma), 5mM Taurine (Sigma), 10 mM 2,3-Butanedione monoxime (Sigma), 0.5 mg ml<sup>-1</sup> collagenase A (Roche) and 0.5 mg ml<sup>-1</sup> collagenase B (Roche) at 37°C. Next, the heart was minced with micro dissecting forceps to dissociate the tissue into single CMs. The cell solution was transferred to Tyrode Buffer supplemented with 1.2 mM CaCl (Sigma) and 5.5 mM D-(+)-Glucose (Sigma) and placed in a Fluorodish for imaging as described above. Rod-like single cells paced at 1 Hz with sharply defined membranes were selected for imaging. All animal care and experimental procedures were approved by the Massachusetts General Hospital Institutional Animal Care and Use Committee.

### Edge Detection

Edge detection was performed by plotting a line intensity profile over the longitudinal axis of the CM in Fiji (Schindelin et al., 2012) where the edge contrast for both the left and right edge was optimal, similar to commonly used edge detection software (Fang et al., 2008). The cell edge was defined as the location of the mean of the maximum and minimum intensity value in the high contrast region of the line profile at the cell edge. The cell length over time was subsequently determined by calculating the distance between the location of the left and right edge of the cell in each frame of a movie.



## **Sarcomere Length Measurement**

Sarcomere length measurement was performed by plotting a line intensity profile in Fiji (Schindelin et al., 2012) over the longitudinal axis of the CM to cover at least 10 sarcomeres, similar to commonly used sarcomere length measurement software (Bub et al., 2010). Due to the alternating dark and light A- and I-bands, the line intensity profile had a sinusoidal appearance. The distance between at least 10 peaks was divided by the number of peaks to reflect the average sarcomere length.

## **Supplemental References**

- Bub, G., Camelliti, P., Bollensdorff, C., Stuckey, D.J., Picton, G., Burton, R.A., Clarke, K., and Kohl, P. (2010). Measurement and analysis of sarcomere length in rat cardiomyocytes in situ and in vitro. *Am J Physiol Heart Circ Physiol* 298, H1616-1625.
- Fang, C.X., Dong, F., Thomas, D.P., Ma, H., He, L., and Ren, J. (2008). Hypertrophic cardiomyopathy in high-fat diet-induced obesity: role of suppression of forkhead transcription factor and atrophy gene transcription. *American journal of physiology Heart and circulatory physiology* 295, H1206-H1215.
- Graham, E.L., Balla, C., Franchino, H., Melman, Y., del Monte, F., and Das, S. (2013). Isolation, culture, and functional characterization of adult mouse cardiomyocytes. *Journal of visualized experiments : JoVE*, e50289.
- Schindelin, J., Arganda-Carreras, I., Frise, E., Kaynig, V., Longair, M., Pietzsch, T., Preibisch, S., Rueden, C., Saalfeld, S., Schmid, B., *et al.* (2012). Fiji: an open-source platform for biological-image analysis. *Nature methods* 9, 676-682.